blood advances

American Society of Hematology
2021 L Street NW, Suite 900,
Washington, DC 20036
Phone: 202-776-0544 | Fax 202-776-0545
bloodadvances@hematology.org

High BM plasma S100A8/A9 is associated with a perturbed microenvironment and poor prognosis in myelodysplastic syndromes

Tracking no: ADV-2022-008958R2

Yu-Hung Wang (National Taiwan University Hospital, Taiwan) Chien-Chin Lin (National Taiwan University Hospital, Taiwan) Chi-Yuan Yao (National Taiwan University Hospital, Taiwan) Fabio Amaral (Cancer Research UK Manchester Institute, United Kingdom) Shan-Chi Yu (National Taiwan University Hospital, Taiwan) Chein-Jun Kao (Cancer Research UK Manchester Institute, United Kingdom) Pin-Tsen Shih (Cancer Research UK Manchester Institute, United Kingdom) Hsin-An Hou (NTUH, Taiwan) Wen-Chien Chou (National Taiwan University Hospital, Taiwan) Hwei-Fang Tien (National Taiwan University Hospital, Taiwan)

Abstract:
S100A8/A9 is a proinflammatory protein and plays an essential role in the pathogenesis of myelodysplastic syndromes (MDS) via the S100A8/A9-Toll-like receptors axis. While S100A8/A9 levels have been used as biomarkers in many inflammatory diseases, their clinical relevance has not been conclusively resolved in MDS. To address this, we used an enzyme-linked immunosorbent assay to quantify S100A8/A9 heterodimers in bone marrow (BM) plasma from 215 MDS patients and compared S100A8/A9 levels across patients with various disease risks and genotypes. S100A8/A9 levels correlated with ASXL1 variant allele frequencies significantly. Moreover, mutant ASXL1 with concurrent RUNX1, STAG2, ZRSR2, or EZH2 mutations was associated with higher S100A8/A9 levels. We further showed that higher S100A8/A9 independently predicted inferior leukemia-free survival and overall survival in MDS patients, irrespective of age, Revised International Prognostic Scoring System subgroups, and known detrimental mutations. Lastly, through deep-sequenced transcriptomic analysis, we demonstrated that higher S100A8/A9 in the BM intimated a perturbed microenvironment with enhanced myeloid-derived suppressor cell-mediated tumor immune escape signal, altered metabolism, and impairment in the functions and quantities of CD8+ T cells and NK cells. S100A8/A9 in the BM microenvironment may be a potential biomarker in the prognostication of MDS and target for novel therapy.

Conflict of interest: No COI declared

COI notes:

Preprint server: No;

Author contributions and disclosures: YHW was responsible for data collection and management, statistical analysis, interpretation, visualization, literature research, and manuscript writing; FA and CYY assisted in bioinformatic analysis and visualization; SCY and PTS helped with sample preparation and processing; HAH and WCC were responsible for data collection and management; and CCL and HFT conceived and coordinated the study and revised the manuscript.

Non-author contributions and disclosures: No;

Agreement to Share Publication-Related Data and Data Sharing Statement: The data reported in this article may be accessed through reasonable requests from the corresponding authors.

Clinical trial registration information (if any):

High BM plasma S100A8/A9 is associated with a perturbed microenvironment and poor prognosis in myelodysplastic syndromes

Short title: S100A8/A9 in myelodysplastic syndrome

Yu-Hung Wang[1,2,3], Chien-Chin Lin[1,4†], Chi-Yuan Yao[1,4,5], Fabio M.R. Amaral[3], Shan-Chi Yu[6], Chein-Jun Kao[3], Pin-Tsen Shih[3], Hsin-An Hou[1], Wen-Chien Chou[1,4], and Hwei-Fang Tien[1,7†]

[1]Division of Hematology, Department of Internal Medicine, National Taiwan University Hospital, Taipei, Taiwan, [2]Division of Cancer Sciences, The University of Manchester, Manchester, United Kingdom, [3]Leukaemia Biology Laboratory, Cancer Research UK Manchester Institute, Manchester, UK, [4]Department of Laboratory Medicine, National Taiwan University Hospital, Taipei, Taiwan, [5]Graduate Institute of Clinical Medicine, College of Medicine, National Taiwan University, Taipei, Taiwan, [6]Department of Pathology, National Taiwan University Hospital, Taipei, Taiwan, [7] Department of Internal Medicine, Far-Eastern Memorial Hospital, New Taipei City, Taiwan

† **Correspondence:** Dr. Chien-Chin Lin, Department of Laboratory Medicine, National Taiwan University Hospital, No. 7, Chung-Shan S. Rd., Taipei City 10002, Taiwan; E-mail: lincc@ntu.edu.tw; Tel: +886-2-23123456;

or Dr. Hwei-Fang Tien, Department of Internal Medicine, National Taiwan University Hospital, No. 7, Chung-Shan S. Rd., Taipei City 10002, Taiwan; E-mail: hftien@ntu.edu.tw; Tel: +886-2-23123456.

Data Sharing

19 The data reported in this article may be accessed through reasonable requests from the

20 corresponding authors: lincc@ntu.edu.tw or hftien@ntu.edu.tw. RNAseq data are available in GEO

21 with access number GSE223305.

22

TO THE EDITOR,

Myelodysplastic syndromes (MDS) represent a heterogeneous group of malignant hematopoietic stem cell (HSC) disorders[1-3]. Recent advances in the immunome of the bone marrow (BM) microenvironment identified aberrant immune activation and proinflammatory signaling as vital drivers in MDS pathogenesis[4-6]. Among these complex networks, the S100A8/A9-Toll-like receptor (TLRs) axis is a critical MDS phenotypes definer[7].

The inflammatory proteins S100A8 and S100A9 often exist as a heterodimer under physiological conditions[8]. In MDS, S100A8/A9 is synthesized and secreted by, among others, myeloid-derived suppressor cells (MDSCs), which play a central role in pathogenesis[9]. The ligation of S100A8/A9 to TLR4 leads to NF-κB-mediated transcription and subsequent production of pro-inflammatory cytokines, and the induction of NLRP3 inflammasome[5,10], which consequently drives pyroptosis of HSCs and an inflammatory milieu in the BM[11,12]. While S100A8/A9 serves as biomarkers in various diseases[13-15], its clinical implication in MDS is not fully deciphered[16].

To investigate the clinical and microenvironmental relevance of S100A8/A9 in MDS patients, we recruited 215 MDS patients at the National Taiwan University Hospital and quantified BM plasma S100A8/A9 dimer levels by Enzyme-linked immunosorbent assay (Supplemental Method). Genomic DNA and mRNA were extracted from BM mononuclear cells and sequenced as previously

described[17,18]. Methods for bioinformatic and statistical analysis are detailed in Supplemental Methods. Patient characteristics are summarized in Table S1. The median age of the patients was 67.5 years. Over a median follow-up duration of 39.7 months, 64 (29.8%) progressed to AML, and 93 patients succumbed to the disease. The National Taiwan University Hospital Research Ethics Committee approved the study (#201709072RINC). Informed consent was obtained in accordance with the Helsinki Declaration.

Correlation analysis revealed that the BM plasma S100A8/A9 protein levels significantly correlated with the mRNA expression in whole BM cell RNA sequencing (r^2=0.32 and r^2=0.31, respectively, Figure S1). We then explored the distribution of S100A8/A9 levels (Figure S2A) across disease subgroups. Patients with MDS/AML (MDS with 10-19% blasts in the BM or peripheral blood) and concurrently mutated *TP53* had higher S100A8/A9 levels than others (Figure S2B). Meanwhile, there was no difference in S100A8/A9 levels among patients in the International Prognostic Scoring System (IPSS) or the Revised IPSS (IPSS-R)[3] subgroups (Figure S2C-F).

Since prior studies demonstrated the impact of genetic events on innate immune and inflammasome-signaling[5], such as the NF-kB pathway[19,20], pyroptosis and β-catenin signaling[21], and NLRP3 inflammatory pathways[7], we examined whether S100A8/A9 concentrations differ across patients with various genotypes. *ASXL1*-mutated patients had significantly higher S100A8/A9 than

those with unmutated *ASXL1* (Figure S2G), while no difference was detected between patients with/without other epigenetic or splicing gene mutations (Figure S2G-H).

Next, we sought to investigate the relationship between mutant *ASXL1* and S100A8/A9 levels. *ASLX1* variant allele frequencies (VAF) significantly correlated with S100A8/A9 levels in 49 *ASXL1*-mutated patients with available VAFs (Figure 1A). Hierarchical clustering suggested close associations among mutations in *ASXL1, STAG2*, *RUNX1*, *EZH2*, and *ZRSR2* (Figure 1B). Interestingly, *ASXL1*-mutated patients with concurrent abovementioned mutations (cluster 1) had a trend of higher S100A8/A9 versus those without (cluster 2) (Figure 1C-D).

The 215 MDS patients were subsequently divided into higher- and lower-S100A8/A9 groups with cutoff point of 7093 ng/mL determined by maximally selected rank statistics. There were no significant differences in the distribution of disease subgroups according to the International Classification Consensus (ICC), IPSS-R, and karyotypes between the two groups, but high-S100A8/A9 patients had a higher *ASXL1* mutation rate (43.5% vs 21.4%) (Table S1-3).

We then examined the impact of S100A8/A9 levels on patients' survival. Higher-S100A8/A9 was associated with significantly inferior leukemia-free survival (LFS) and overall survival (OS) not only in the total cohort (Figure 1E), but also in the lower- and higher-risk subgroups based on the ICC and IPSS-R (Figure 1F-G and Figure S3-4). Time-dependent ROC curve analysis also suggested the

potential for S100A8/A9 to supplement IPSS-R (Figure 1H). Moreover, despite having higher frequencies of mutant *ASXL1*, high-S100A8/A9 patients had poorer survival than the lower-S100A8/A9 group irrespective of *ASXL1* mutation statuses (Figure 1I and Figure S5).

The prognostic implications of S100A8/A9 levels on survival were also demonstrated in patients carrying different karyotypes (Figure S6) or receiving different treatments (Figure S7). Remarkably, in 50 patients who received hypomethylating agent monotherapy, higher-S100A8/A9 retained strong discriminatory prognostic impact on LFS and OS (Figure S8). In multivariable analysis, we included parameters with a *p*-value <0.05 in the univariate analysis (Table S4), and hazard ratios were adjusted with treatments that well-stratified survivals (Figure S9). Higher-S100A8/A9 remained an independent adverse prognostic factor for LFS and OS (Figure 2A).

Considering that RNAseq was performed on whole BM MNCs, we referenced the single-cell dataset of healthy controls[22] to identify which cell types contributed to the differentially expressed genes. Curiously, 18 of the 20 most down-regulated genes (Table S5) in high-S100A8/A9 BM were regularly expressed by lymphocytes (Figure S10), implying different composition of lymphocytes in higher- and lower-S100A8/A9 BMs. We further adopted CIBERSORTx[18,23], which infers the landscape of infiltrating immunocytes in the BM from gene expression profiles. Higher-S100A8/A9 was associated with significantly lower fractions of CD8 T-cells and activated NK-cells (Figure 2B and Table S6).

Weighted gene co-expression network analysis revealed that the turquoise and blue modules were closely associated with lower- and higher-S100A8/A9, respectively (Figure S11). Corresponding to CIBERSORTx analysis, the 914 genes in the turquoise module were enriched in pathways involving NK- and T-cell functions, while the 509 genes in the blue module were enriched in pathways involving MDSCs in cancer immune escape and altered metabolism (Figure 2C-D).

To the best of our knowledge, this is the first study to significantly stratify MDS patients' survival based on S100A8/A9 levels. We also observed that *ASXL1*-mutated patients had higher S100A8/A9 concentrations than their unmutated counter partners, corresponding with the increase in NADPH oxidase and ROS, TLR4 activation and pyroptosis[7]. Fundamentally, the upregulation of S100A8/A9 can exert genotoxic stress in HSCs, thereby advancing the risk for AML transformation[24], in accordance with our finding that higher-S100A8/A9 group had a shorter LFS. In a homogeneously treated lower-risk MDS cohort, S100A8/A9 expression in mesenchymal stem cells was correlated with p53 and TLR4 upregulation[24]. Additionally, high S100A8/A9 concentrations doubled the risk of leukemic transformation and significantly reduced the time to AML transformation.

Comparisons of the transcriptomic data highlighted differences in functions and properties of immune cells between higher- and lower-S100A8/A9 BM and suggested a high-risk sub-entity, which was not considered in current risk stratification, in this heterogenous disease and required

more attention. However, the lack of external validation, biological validation, and the assessment of the impact of other inflammasome components, such as cytokines or chemokines, is a major issue. Meanwhile, the demographics of our MDS population are more similar to Korean patients[25], with a younger and higher-risk skewing when compared to western cohorts, suggesting that the extrapolation of our data may be compromised. Treatment heterogeneity could also potentially confound our analysis. Serial follow-up data after treatment will strengthen the prognostic power of S100A8/A9 and provide more insight into the changes in the BM microenvironment. Additionally, our findings could be more granular and justified if cytometry by time of flight or single-cell multi-omics approaches were adopted.

Despite above limitations, this study clearly showed that S100A8/A9 level was an independent poor prognostic factor in MDS, and higher S100A8/A9 in the BM intimated a perturbed microenvironment with enhanced MDSC signal and impairment in the functions and quantities of CD8+ T cells and NK cells. We propose S100A8/A9 can be incorporated to current risk stratification systems and prospectively assessed in clinical trials.

Acknowledgements

We acknowledge the service provided by Department of Laboratory Medicine, Department of Medical Research, and Division of Hematology, Department of Internal Medicine, National Taiwan University Hospital. We also appreciate Dr Joanna Storer's help with English editing. FMRA was supported by Cancer Research UK grant number C5759/A27412.

Authorship Contributions

YHW was responsible for data collection and management, statistical analysis, interpretation, visualization, literature research, and manuscript writing; FA and CYY assisted in bioinformatic analysis and visualization; SCY and PTS helped with sample preparation and processing; HAH and WCC were responsible for data collection and management; and CCL and HFT conceived and coordinated the study and revised the manuscript.

Competing Interests statement: The authors declare that they have no competing interests.

Funding: The work was supported by grants from Ministry of Science and Technology, Taiwan, project number: MOST 109-2314-B-002-221, 109-2314-B-002-222; and Taiwan Ministry of Health and Welfare, project number: MOHW109-TDU-B-211-134009. FMRA is funded by Cancer Research UK grant number C5759/A27412.

Reference

1. Khoury JD, Solary E, Abla O, et al. The 5th edition of the World Health Organization Classification of Haematolymphoid Tumours: Myeloid and Histiocytic/Dendritic Neoplasms. *Leukemia*. 2022;36(7):1703-1719.
2. Arber DA, Orazi A, Hasserjian RP, et al. International Consensus Classification of Myeloid Neoplasms and Acute Leukemia: Integrating Morphological, Clinical, and Genomic Data. *Blood*. 2022.
3. Greenberg PL, Tuechler H, Schanz J, et al. Revised international prognostic scoring system for myelodysplastic syndromes. *Blood*. 2012;120(12):2454-2465.
4. Barreyro L, Chlon TM, Starczynowski DT. Chronic immune response dysregulation in MDS pathogenesis. *Blood*. 2018;132(15):1553-1560.
5. Sallman DA, List A. The central role of inflammatory signaling in the pathogenesis of myelodysplastic syndromes. *Blood*. 2019;133(10):1039-1048.
6. Winter S, Shoaie S, Kordasti S, Platzbecker U. Integrating the "Immunome" in the Stratification of Myelodysplastic Syndromes and Future Clinical Trial Design. *Journal of Clinical Oncology*. 2020;38(15):1723-1735.
7. Basiorka AA, McGraw KL, Eksioglu EA, et al. The NLRP3 inflammasome functions as a driver of the myelodysplastic syndrome phenotype. *Blood*. 2016;128(25):2960-2975.
8. Wang S, Song R, Wang Z, Jing Z, Wang S, Ma J. S100A8/A9 in Inflammation. *Front Immunol*. 2018;9:1298.
9. Chen X, Eksioglu EA, Zhou J, et al. Induction of myelodysplasia by myeloid-derived suppressor cells. *J Clin Invest*. 2013;123(11):4595-4611.
10. Sallman DA, Cluzeau T, Basiorka AA, List A. Unraveling the Pathogenesis of MDS: The NLRP3 Inflammasome and Pyroptosis Drive the MDS Phenotype. *Front Oncol*. 2016;6:151.
11. Ratajczak MZ, Bujko K, Cymer M, et al. The Nlrp3 inflammasome as a "rising star" in studies of normal and malignant hematopoiesis. *Leukemia*. 2020;34(6):1512-1523.
12. Cluzeau T, McGraw KL, Irvine B, et al. Pro-inflammatory proteins S100A9 and tumor necrosis factor-α suppress erythropoietin elaboration in myelodysplastic syndromes. *Haematologica*. 2017;102(12):2015-2020.
13. van Zoelen MA, Vogl T, Foell D, et al. Expression and role of myeloid-related protein-14 in clinical and experimental sepsis. *Am J Respir Crit Care Med*. 2009;180(11):1098-1106.
14. Austermann J, Friesenhagen J, Fassl SK, et al. Alarmins MRP8 and MRP14 induce stress tolerance in phagocytes under sterile inflammatory conditions. *Cell Rep*. 2014;9(6):2112-2123.
15. Pruenster M, Vogl T, Roth J, Sperandio M. S100A8/A9: From basic science to clinical application. *Pharmacol Ther*. 2016;167:120-131.
16. Giudice V, Wu Z, Kajigaya S, et al. Circulating S100A8 and S100A9 protein levels in plasma of patients with acquired aplastic anemia and myelodysplastic syndromes. *Cytokine*. 2019;113:462-465.

193 17. Tsai CH, Hou HA, Tang JL, et al. Prognostic impacts and dynamic changes of cohesin complex
194 gene mutations in de novo acute myeloid leukemia. *Blood Cancer J*. 2017;7(12):663.
195 18. Wang Y-H, Hou H-A, Lin C-C, et al. A CIBERSORTx-based immune cell scoring system could
196 independently predict the prognosis of patients with myelodysplastic syndromes. *Blood Advances*.
197 2021;5(22):4535-4548.
198 19. Choudhary GS, Pellagatti A, Agianian B, et al. Activation of targetable inflammatory immune
199 signaling is seen in myelodysplastic syndromes with SF3B1 mutations. *eLife*. 2022;11:e78136.
200 20. Lee SC, North K, Kim E, et al. Synthetic Lethal and Convergent Biological Effects of
201 Cancer-Associated Spliceosomal Gene Mutations. *Cancer Cell*. 2018;34(2):225-241.e228.
202 21. Zhang Q, Zhao K, Shen Q, et al. Tet2 is required to resolve inflammation by recruiting Hdac2 to
203 specifically repress IL-6. *Nature*. 2015;525(7569):389-393.
204 22. Granja JM, Klemm S, McGinnis LM, et al. Single-cell multiomic analysis identifies regulatory
205 programs in mixed-phenotype acute leukemia. *Nature Biotechnology*. 2019;37(12):1458-1465.
206 23. Newman AM, Steen CB, Liu CL, et al. Determining cell type abundance and expression from
207 bulk tissues with digital cytometry. *Nature Biotechnology*. 2019;37(7):773-782.
208 24. Zambetti NA, Ping Z, Chen S, et al. Mesenchymal Inflammation Drives Genotoxic Stress in
209 Hematopoietic Stem Cells and Predicts Disease Evolution in Human Pre-leukemia. *Cell Stem Cell*.
210 2016;19(5):613-627.
211 25. Lee JH, Jang JH, Park J, et al. A prospective multicenter observational study of decitabine
212 treatment in Korean patients with myelodysplastic syndrome. *Haematologica*.
213 2011;96(10):1441-1447.

214

215

Figure legends

Figure 1.

(A) Scatter plots showed a moderate correlation between *ASXL1* variant allele frequencies and S100A8/A9 levels.

(B) Heatmap of correlations among mutations.

(C) Clustering 51 *ASXL1*-mutated patients based on concurrent mutations of *STAG2*, *RUNX1*, *EZH2*, and *ZRSR2.*

(D) Cluster 1 had a trend of higher S100A8/A9 levels than cluster 2.

(E) Higher S100A8/A9 conferred inferior leukemia-free survival (LFS) and overall survival (OS) of the 215 MDS patients.

(F) Higher S100A8/A9 conferred significantly worse OS in International Classification Consensus lower-risk group and higher-risk group. Higher-risk: MDS with excess blast and MDS/AML; and lower-risk: others.

(G) Higher S100A8/A9 conferred significantly shorter OS in IPSS-R lower-risk (very low, low, and intermediate) group and a trend of worse OS in IPSS-R higher-risk (IPSS-R high and very high) group.

(H) Time-dependent ROC curve analyses demonstrate that S100A8/A9 levels can be complementary to IPSS-R, increasing area under curves when incorporated.

(I) Patients with higher S100A8/A9 had significantly inferior OS irrespective of their *ASXL1* mutation statuses.

Figure 2.

(A) Multivariable analysis for leukemia-free survival (LFS) and overall survival (OS). Statistically significant if $P \leq 0.007$ (adjusted by Bonferroni correction).

Abbreviations: HR, hazard ratios; CI, confidence interval.

*As continuous variable analysis.

†IPSS-R risk groups: Very low, low, intermediate, high, very high.

‡High vs. low S100A8/A9.

§adjusted with different treatments: supportive care only, hematopoietic stem cell transplant (HSCT) with/without any other treatment, hypomethylating agent with/without other chemotherapies but HSCT, and all other treatments.

Note: only variables with P value less than or equal to 0.05 in univariate analysis were incorporated into the multivariable Cox proportional hazard regression analysis.

(B) CIBERSORTx analysis revealing significant differences in the fractions of specific cell types between higher- and lower-S100A8/A9 BM. There were higher proportions of activated CD4 T-cells, CD8 T-cells, NK-cells, and naïve B-cells in the lower-S100A8/A9 BM while the fractions of naïve CD4 T-cell, resting mast cells, monocytes, and neutrophils were higher in the higher-S100A8/A9 BM.

(C&D). Bar charts showed 10 robustly enriched functional pathways in lower-S100A8/A9 (C) and higher-S100A8/A9 (D) BMs, respectively.

Figure 1

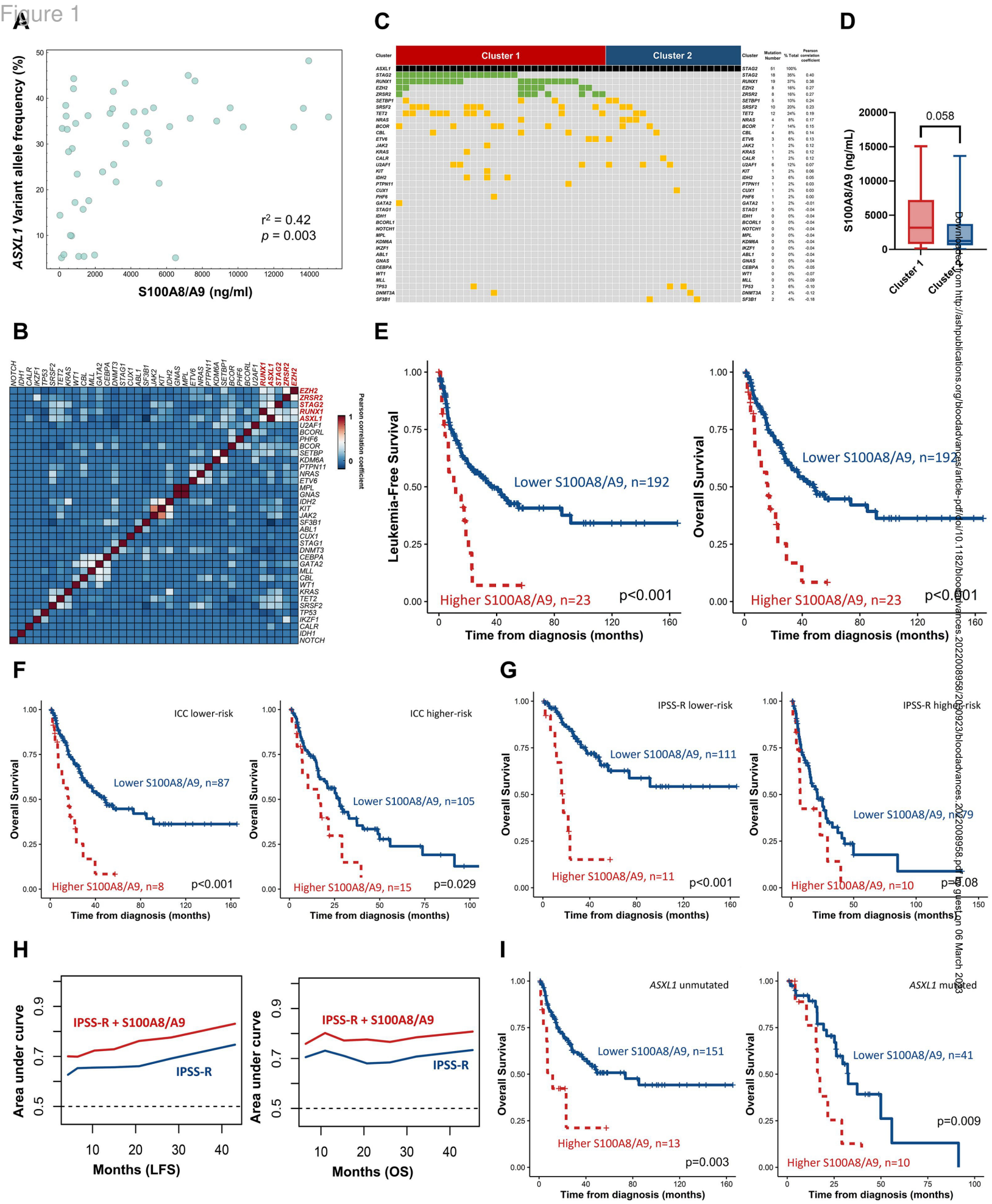

Figure 2

A

	LFS				OS			
		95% CI				95% CI		
Variable	HR§	Lower	Upper	*P*	HR§	Lower	Upper	*P*
Age*	1.020	1.005	1.034	0.007	1.029	1.013	1.046	<0.001
IPSS-R†	1.425	1.153	1.761	0.001	1.616	1.282	2.037	<0.001
RUNX1	1.433	0.819	2.509	0.208	1.492	0.824	2.701	0.187
SF3B1	0.654	0.346	1.236	0.191	0.667	0.335	1.330	0.250
STAG2	0.832	0.449	1.542	0.559	0.912	0.485	1.717	0.776
TP53	3.552	2.000	6.310	<0.001	6.244	3.290	11.849	<0.001
Higher S100A8/A9‡	2.405	1.346	4.299	0.003	2.279	1.248	4.162	0.007

B

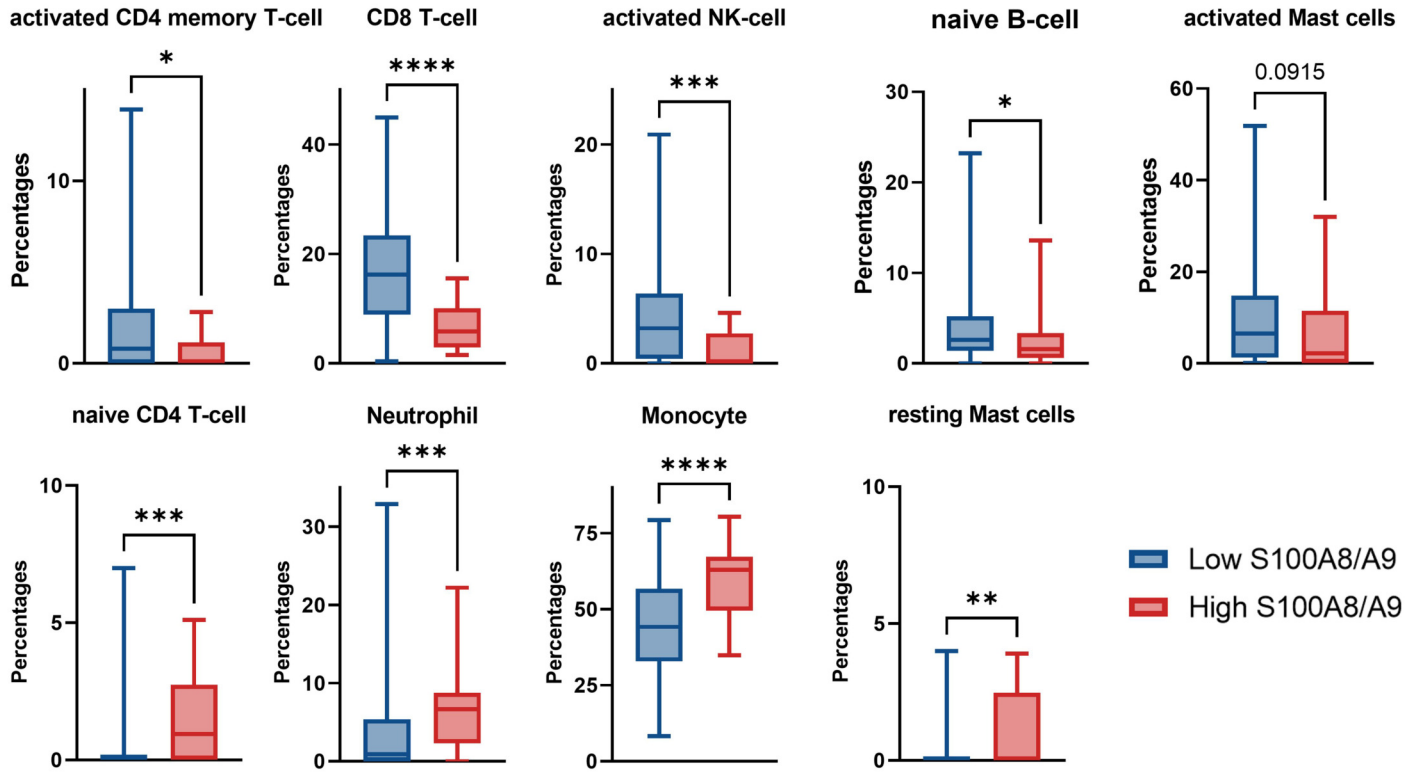

C

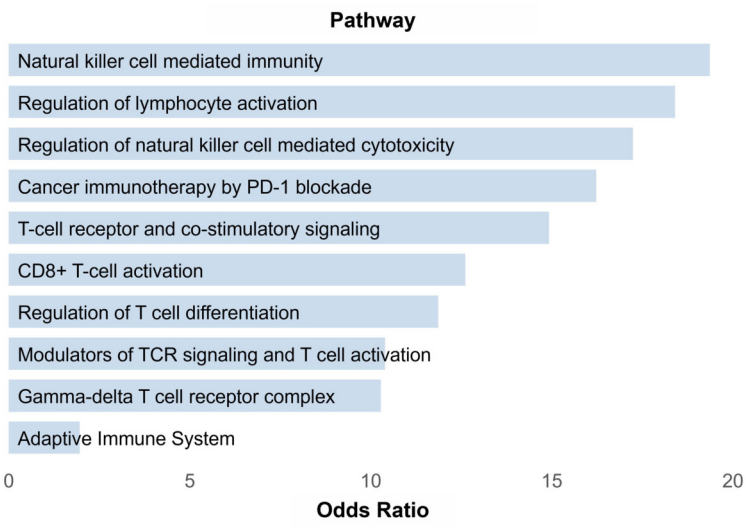

D